Stanford Exploration Project, Report 67, January 13, 1998, pages 1–119

Correlation-picking deconvolution

Carlos A. Cunha Filho[1]

keywords: *wavelet, deconvolution, reflectivity*

ABSTRACT

A scaled correlation between the residuals and the wavelet is used as the basis of a new deconvolution approach, which resolves first the strongest events and then, as the number of iteration increases, the weaker events of the reflectivity sequence. An important property of this method is that the retrieved series has the same frequency content as the original sequence. The results obtained with the application of this algorithm to real data are equivalent to a sharper version of the results of predictive deconvolution.

INTRODUCTION

The spectra of the reflectivity series estimated by most deconvolution methods is usually constrained by the band-limited spectrum of the original wavelet. Because of this constraint, the reflectivity series retrieved by those methods actually correspond to a lower-frequency version of the true reflectivity series. Several methods have been proposed to overcome the adverse effects of this band limitation, such as minimum-entropy deconvolution (Wiggins, 1978), relative-entropy deconvolution (Jacobs and van der Geest, 1988) and L_p-norm deconvolution (Debeye and van Riel, 1989).

I derive an alternative approach to this problem and and analyze its results in synthetic and real data. This approach is an iterative deconvolution process, that is based on the picking of absolute maxima of the absolute values of a scaled correlation between the residuals and the wavelet, within a pre-specified range (related to the wavelet length). An important property of the proposed method is that the spectrum of the retrieved reflectivity series shows the same frequency distribution as the original reflectivity sequence.

[1]**email:** not available

The method is defined first for the simple case, of a known wavelet. In this case, if the reflectivity sequence is sufficiently sparse, the method finds the exact solution in a few iterations. As the reflectivity series becomes less sparse, the number of required iterations increases until it reaches the point where it is unable to find the exact solution within a finite number of iterations. Because of its slow rate of convergence, I combine the method with the usual least-squares inversion after some iterations, to speed up the process.

For the more interesting case of an unknown wavelet, the method requires an initial estimation of the wavelet to start the iterative scheme; the final solution depends on this initial choice. The results obtained when the method is applied to a deep-water CMP gather correspond to a slightly sharper version of the results obtained with predictive deconvolution.

DECONVOLUTION WITH A KNOWN WAVELET

Let's first address the problem of retrieving the reflectivity series when the wavelet is known. Our problem is to find the series $\mathbf{r}$, from the recorded series

$$\mathbf{t} = \mathbf{w} * \mathbf{r}, \tag{1}$$

where $\mathbf{w}$ is the known wavelet.

The basic operator

If we consider the simple case in which $\mathbf{r}$ is a sufficiently sparse series (so that the number of samples between any two adjacent non-zero-valued samples is at least equal to the number of samples of the wavelet, i.e. L_w), it is possible to devise a simple operator to retrieve $\mathbf{r}$:

$$\mathbf{r} = \mathbf{P_w}\{\mathbf{t}\} = \delta^{2L_w-1}\{\frac{\mathbf{w} \star \mathbf{t}}{\parallel \mathbf{w} \parallel^2}\}. \tag{2}$$

The symbol $\star$ stands for correlation, while the operator $\delta^{\mathbf{L}}$ is defined as follows: The result of

$$\mathbf{r} = \delta^L\{\mathbf{c}\}$$

is given by

$$r_i = \delta_i^L c_i$$

where

$$\delta_i^L = \begin{cases} 1 & \text{if } c_i \text{ is an absolute maximum of the series of absolute values of } \mathbf{c} \text{ inside a window of } L \text{ sam-. ples, centered in } c_i \\ 0 & \text{otherwise.} \end{cases}$$

When the series $\mathbf{r}$ is still sparse but the temporal distance between non-vanishing-samples is larger than the minimum distance still resolvable by the wavelet (that is $dt \geq 1/[2f]$, where f is the highest frequency component of the wavelet), the operator in equation (2) will not give the exact solution. Here however, an exact solution can still be obtained through an iterative process. Let's consider equation (2) as the zero-order approximation $\mathbf{r^0}$ to the time series $\mathbf{r}$:

$$\mathbf{r^0} = \delta^{2L_w-1}\{\frac{\mathbf{w} \star \mathbf{t}}{\| \mathbf{w} \|^2}\}. \tag{3}$$

The residual between the original trace and the trace predicted by this zero-order approximation for the reflectivity will be

$$\mathbf{\Delta t^0} = \mathbf{t} - \mathbf{t^0} = \mathbf{w} * (\mathbf{r} - \mathbf{r^0}). \tag{4}$$

Because the operator $\mathbf{P_w}$ in equation (2) is an approximation to the inverse of the convolution by $\mathbf{w}$, we can apply it to equation (4) to get a zero-order approximation to $\mathbf{r} - \mathbf{r^0}$:

$$\mathbf{\Delta r^0} = \mathbf{r} - \mathbf{r^0} = \mathbf{P_w}\{\mathbf{\Delta t^0}\}. \tag{5}$$

Therefore, the first-order approximation for the reflectivity series will be

$$\mathbf{r^1} = \mathbf{r^0} + \mathbf{\Delta r^0},$$

and in general

$$\mathbf{r^i} = \mathbf{r^{i-1}} + \mathbf{P_w}\{\mathbf{t} - \mathbf{t^{i-1}}\} = \mathbf{r^{i-1}} + \mathbf{P_w}\{\mathbf{t} - \mathbf{w} * \mathbf{r^{i-1}}\}. \tag{6}$$

In Figure 1 this iterative process is applied to a synthetic trace whose original reflectivity series is comprised of sparse spikes. The distance between some of the spikes is successively decreased to show how the relaxation of the sparseness condition affects the convergence of the method. Except for *(c)*, the exact solution was reached in a few number of iterations, even when the separation between adjacent spikes is reduced to one third of the wavelet size. Because in *(c)* the exact solution was not reached within a finite number of iterations (though an extremely close solution was found after a few iterations), it will be necessary to improve the basic operator P_w if we intend to apply the method to more complex time series.

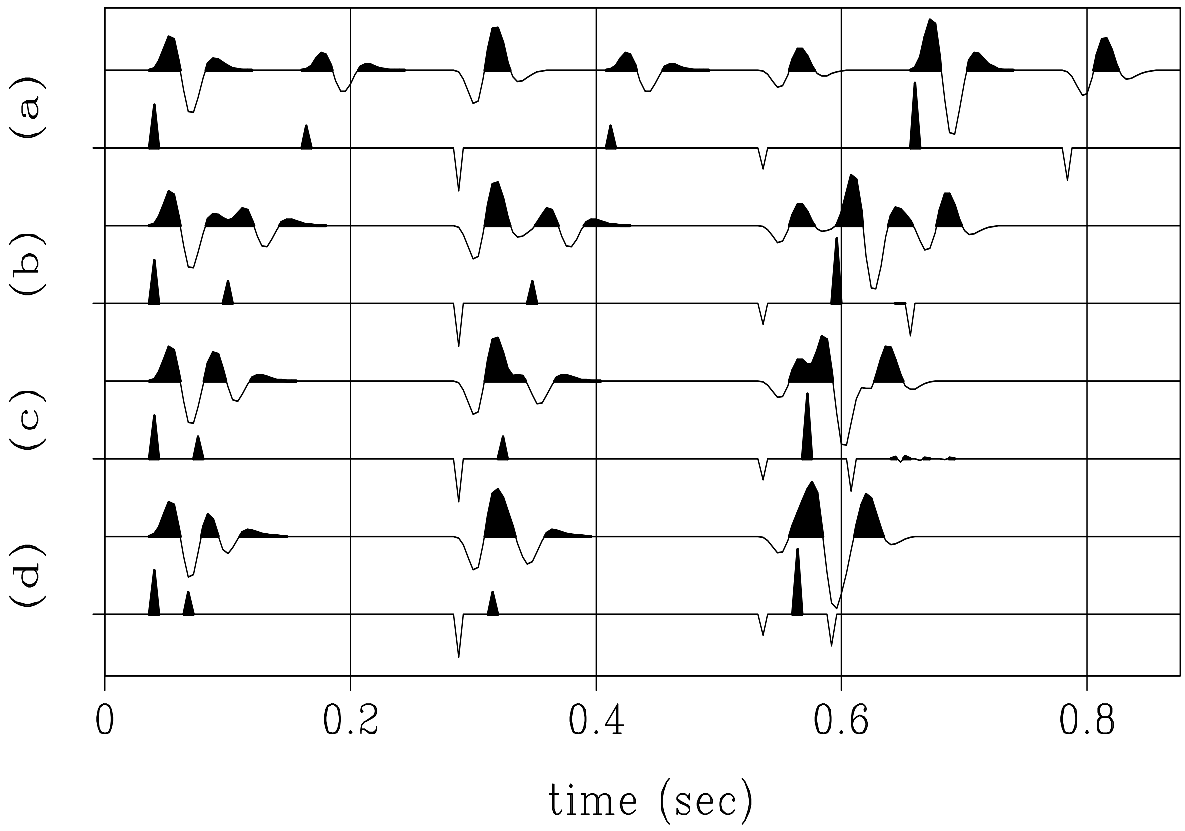

Figure 1: The iterative process described by equation (6) is applied to four synthetic traces. The traces differ only in the distance between some of the spikes of the associated reflectivity series. *(a)* When the distance between spikes is around 1.5 times the wavelet's size the exact reflectivities are retrieved on the 0-order iteration (that is, equation 2). As the distance between some of the spikes decreases, the number of iterations necessary to get the exact solution increases: 1 iteration in *(b)* and 8 iterations in *(d)*. Although *(c)* has a fast convergence (the sixth iteration is shown), the exact solution is not reached, as we can see by the small residuals beyond 0.6 seconds. carlos1-sparse [NR]

Building a more complex operator

Both low- and high-frequency components of the reflectivity series will not be correctly resolved by the iterative process described by equation (6). When two adjacent reflectivities with the same polarity are sufficiently close, they will not be represented by distinguishable peaks in the correlation series. The method will "see" a single reflectivity, with an amplitude close to the sum of the amplitudes of the two actual reflectivities. Similarly, if two close, adjacent reflectivities have opposite polarity, the scaled correlation will still show two peaks but with amplitudes smaller than the amplitudes of the original reflectivities.

One way to avoid the excessive influence of the initial picking steps (which is crucial to retrieve the lower-frequency components of the reflectivity) is to introduce a damping factor in equation (6)

$$\mathbf{r^i} = \lambda\, \mathbf{r^{i-1}} + \mathbf{P_w}\{\mathbf{t} - \mathbf{w} * \lambda\, \mathbf{r^{i-1}}\}. \tag{7}$$

Although fast on the beginning, the convergence rate tends slow after the initial iterations. To overcome this problem I use a least-squares inversion of the residuals after a specified number of iterations of the method. I formulate the least-squares problem so that the objective function to be minimized is

$$\mathbf{O} = \parallel \mathbf{\Delta t^m} - \mathbf{w} * \mathbf{\Delta r^m} \parallel^2, \tag{8}$$

where $\mathbf{t^m}$ are the residuals of the last iteration of the method, and $\mathbf{\Delta r^m}$ are the unknowns. The final estimated reflectivities will be given by

$$\mathbf{r_f} = \mathbf{r^m} + \mathbf{\Delta r^m}. \tag{9}$$

As suggested by Claerbout (1989), to generate a sparse synthetic sequence, we can take an integer power of a series comprised of Gaussian noise. I used the third power to build a synthetic reflectivity sequence, because it represents about the limit of resolution for wavelet estimation (for a white-spectrum wavelet). Figures 2 and 3 show a comparison between different approaches used to deconvolve the synthetic trace.

We can see from Figure 2 that when the basic operator is used *(c)* most of the major events are correctly recovered, but the low-frequency components of the reflectivities are not properly resolved (e.g., the negative event between 0.3 and 0.4 seconds). When a damping factor of 0.5 is introduced *(d)* the low-frequency components of the original reflectivity are better retrieved but the high-frequency components are still unresolved, as we can see by the events beyond 0.6 seconds. These events are better resolved in the last trace of this figure *(e)*, which refers to the least-squares residual inversion applied to *(d)*.

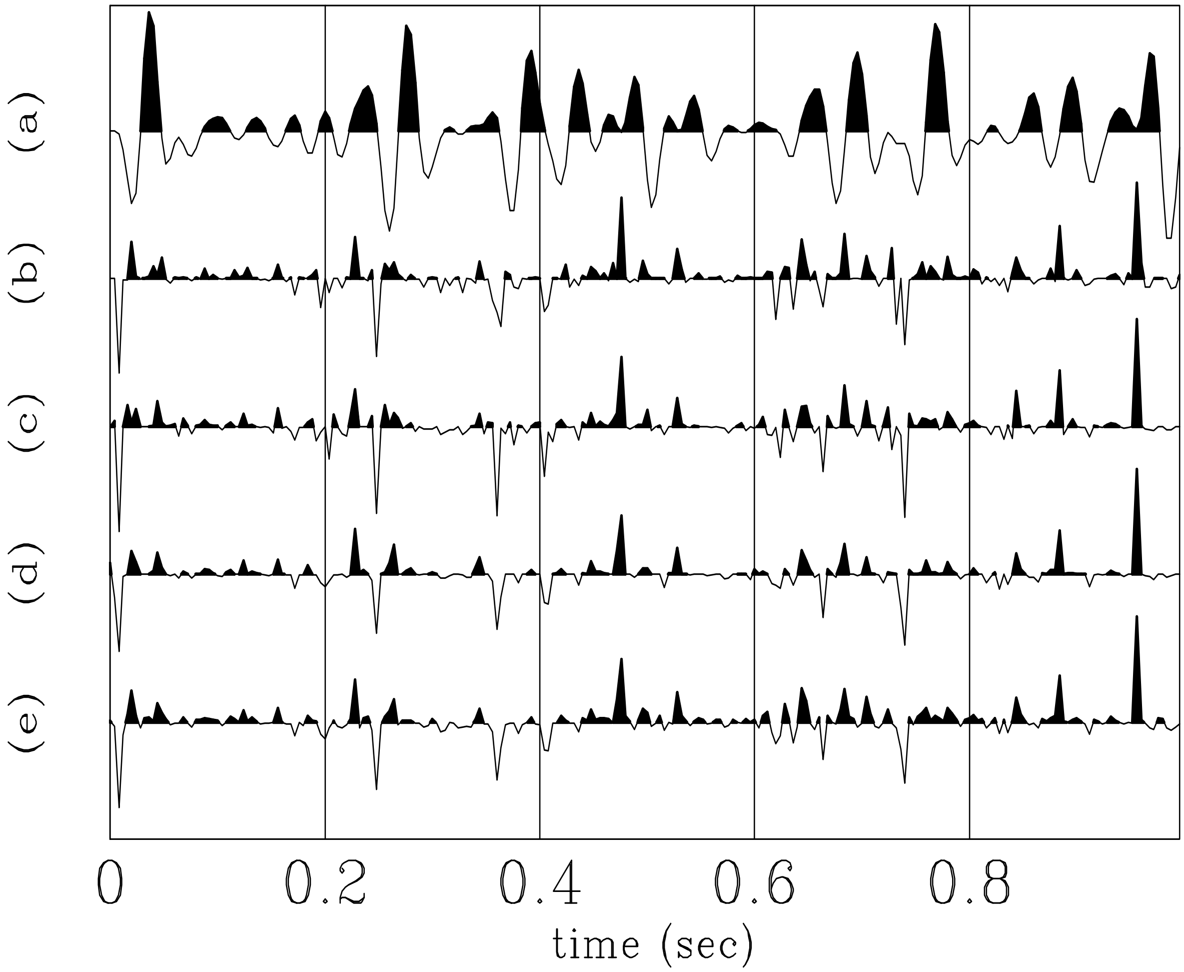

Figure 2: *(a)* the synthetic trace generated by the convolution of the wavelet (a minimum-phase Ricker) with the synthetic reflectivity series *(b)*, obtained by taking the third power of a Gaussian noise sequence. The other three traces correspond to the reflectivities retrieved by different versions of the iterative correlation-picking decon. *(c)* corresponds to the basic operator described by equation (6); in *(d)* a damping factor of 0.5 was introduced according to equation (7); and in *(e)* an extra residual-least-squares step is applied on the output of the damped operator as in equation (9). All cases correspond to 250 iterations, which is the number of samples. carlos1-knowt1 [NR]

Figure 3 shows a comparison between the reflectivity series retrieved by different methods: predictive deconvolution in *(b)*, convolution with the least-squares inverse of the wavelet in *(c)*, direct least-squares inversion in *(d)*, and the least-squares applied to the residuals of the damped, iterative correlation-picking decon *(e)* , which is the same as *(e)* in Figure 2. The direct least-squares and the correlation-picking deconvolutions correspond to the sequences that better fit the original series *(a)*. It is clear, however, that the iterative correlation-picking (ICP) result has the same frequency content as the original sequence, while the least-squares inversion (LSI) corresponds to its lower-frequency version.

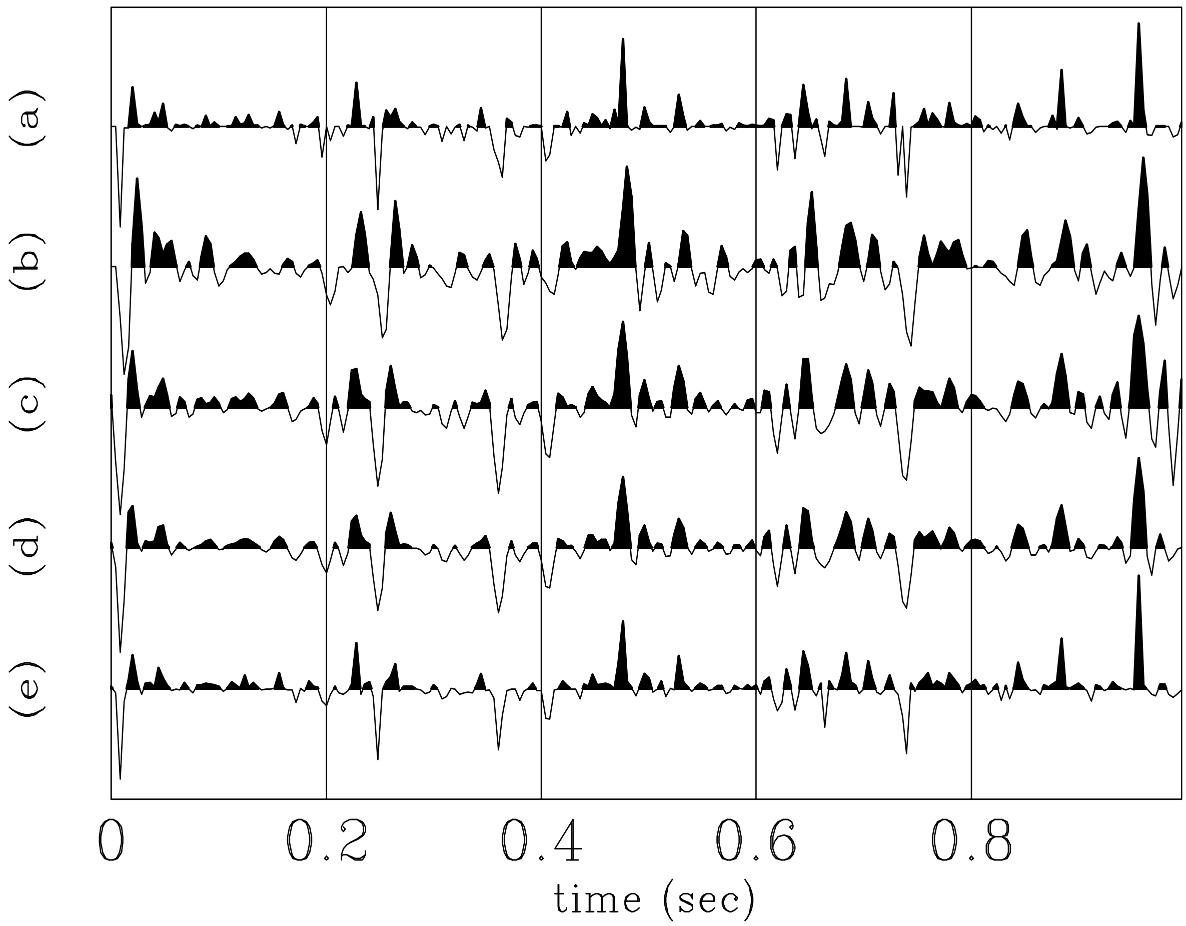

Figure 3: *(a)* corresponds to the original (true) reflectivity sequence (as Figure 2-*b*); the other traces are the reflectivity series retrieved by different algorithms: *(b)* is the result of the predictive deconvolution (plotted with a scale factor of 13); while in *(c)* a least-squares inversion was performed for the known wavelet and the resulting inverse filter convolved with the original trace (Figure 2-*a*). *(d)* corresponds to the result of the direct least-squares inversion of the original trace (plotted with a scale factor of 1.45), and *(e)* is the reflectivity series retrieved by the ICP algorithm with a residual least-squares step (as in Figure 2-*e*). carlos1-knowt2 [NR]

The spectra of the synthetic trace, the original reflectivity series, and the reflectivities recovered by each of the methods described in Figure 3, are shown in Figure 4. In the central frequency range of the original wavelet (10-50 Hz) all methods, except the predictive decon, correctly recover the shape of the reflectivity spectrum. Since the predictive decon does not use any information regarding the original wavelet (except that it is minimum-phase), its relative weakness compared to other methods would be expected. In the low-frequency region however, only the ICP and LSI algorithms properly retrieve the shape of the original reflectivities. All methods, except the ICP, show a decay for high frequencies that follows the same decay pattern of the trace (and wavelet) spectrum. That is why, although with the same shape, the spectra retrieved by those methods have a higher amplitude than the spectrum of the true reflectivities in the low and medium range of frequency.

The ICP algorithm, however, keeps the same amplitude level in the whole frequency domain, with two direct consequences: it exactly recovers both the shape and the amplitude of the original spectrum in the range of frequencies covered by the wavelet, and it loosely recovers the part of the spectrum that is not covered by the wavelet. This result is better than just zero this part of the spectrum.

Final comparisons between the LSI and ICP algorithms are presented in Figures 5 and 6. In the first of these figures, I show that when the ICP algorithm with a residual least-squares step is used, the residuals ($\Delta\mathbf{t}$) are smaller than those of the LSI algorithm. In Figure 6 I compare the impedance profiles obtained from these two algorithms with the impedance obtained from the original reflectivity series. The impedance obtained with the ICP method shows a slightly better fitting of the true impedance, than the one obtained with the LSI method.

A generalization for the δ^L operator

Although I have not yet explored the practical implications of this, the operator δ^L, previously defined, can be described as a particular case of a more general operator $\mathcal{D}_L^\alpha$:

$$\mathbf{r} = \mathcal{D}_L^\alpha\{\mathbf{c}\} \quad \longrightarrow \quad r_i = \frac{c_i^\alpha}{\sum_{j=i-n}^{i+n} \mid c_j^\alpha \mid}, \tag{10}$$

where $\qquad n = \dfrac{L+1}{2}, \qquad$ and $\qquad \alpha \qquad$ is any odd integer.

The operator δ^L can be defined as

$$\delta^L = \lim_{\alpha\to\infty} \mathcal{D}_L^\alpha. \tag{11}$$

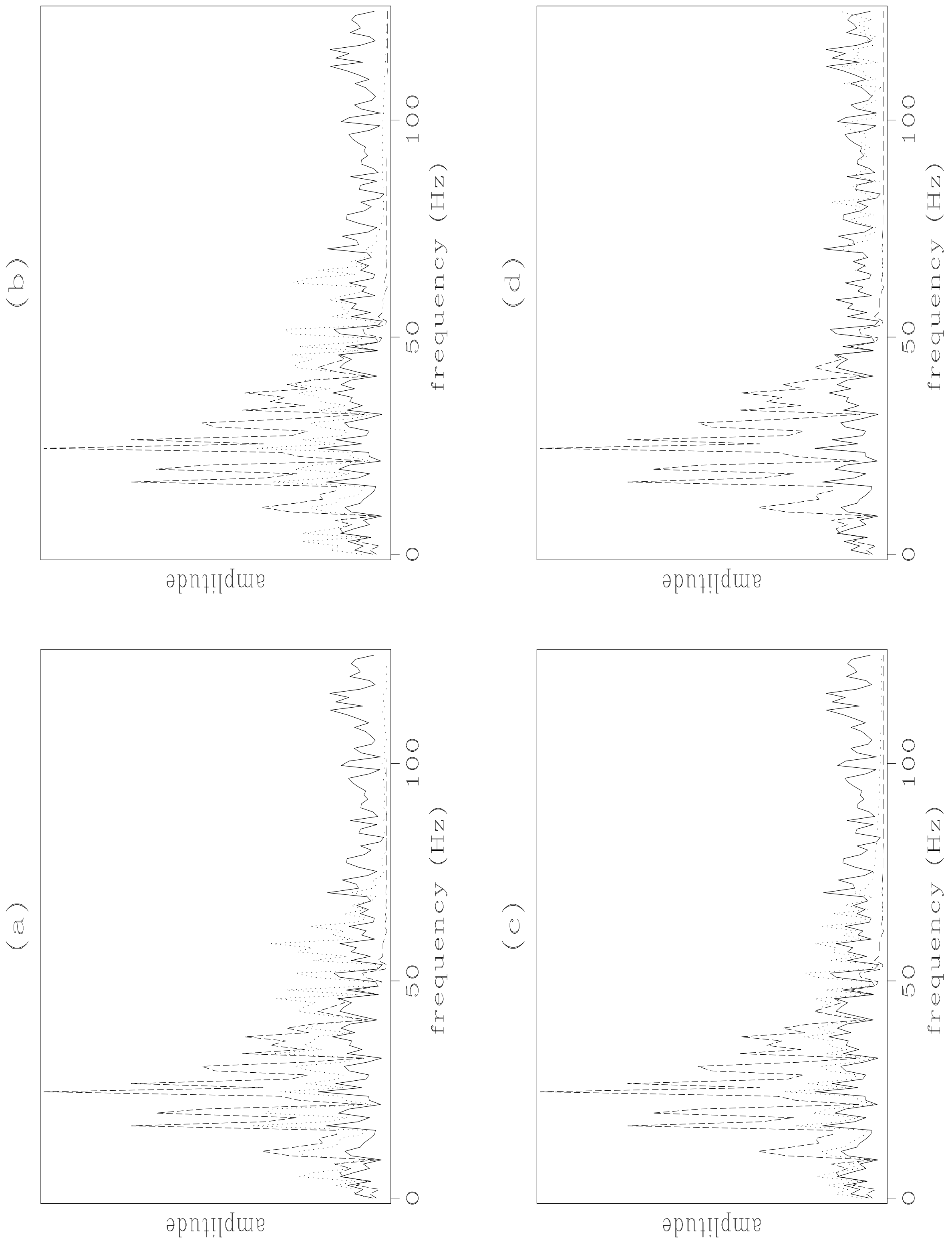

Figure 4: In all graphs the **dashed** line corresponds to the spectrum of the original trace, the **continuous** line corresponds to the spectrum of the original reflectivity sequence, and the **dotted** line applies for the spectra of the retrieved reflectivity sequences of Figure 3 *b-e*. *(a)* predictive decon, *(b)* convolution with least-squares inverse wavelet filter, *(c)* LSI algorithm, and *(d)* ICP with residual least-squares step. carlos1-knows [NR]

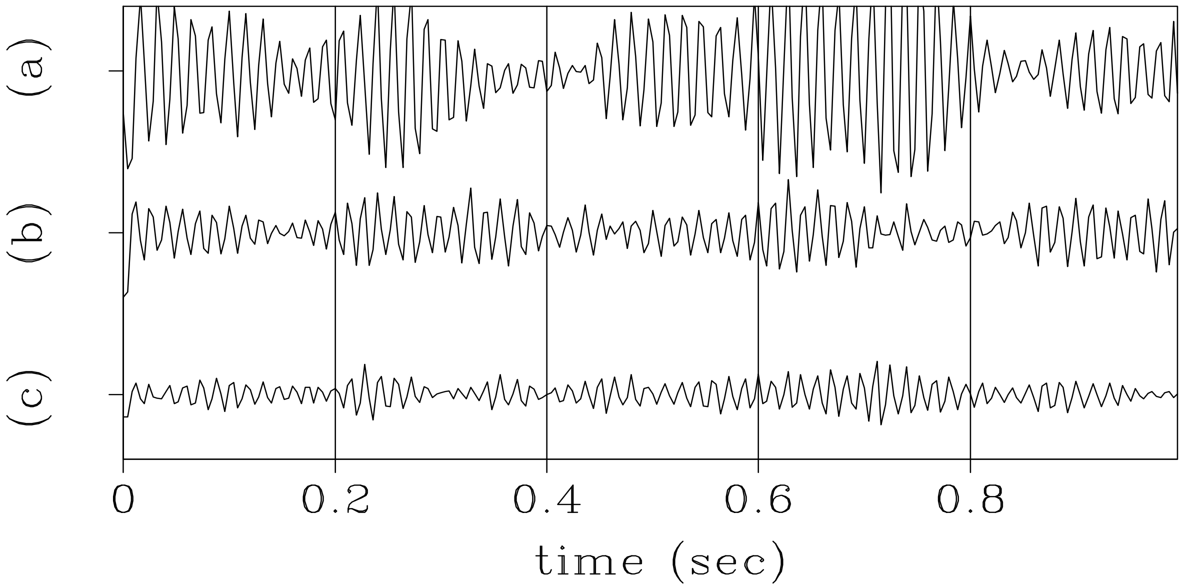

Figure 5: *(a)* Residuals of the damped ICP algorithm after 25,000 iterations, *(b)* residuals of the LSI algorithm, and *(c)* residuals of the damped ICP with residual least-squares algorithm after 250 iterations. carlos1-knowdif [NR]

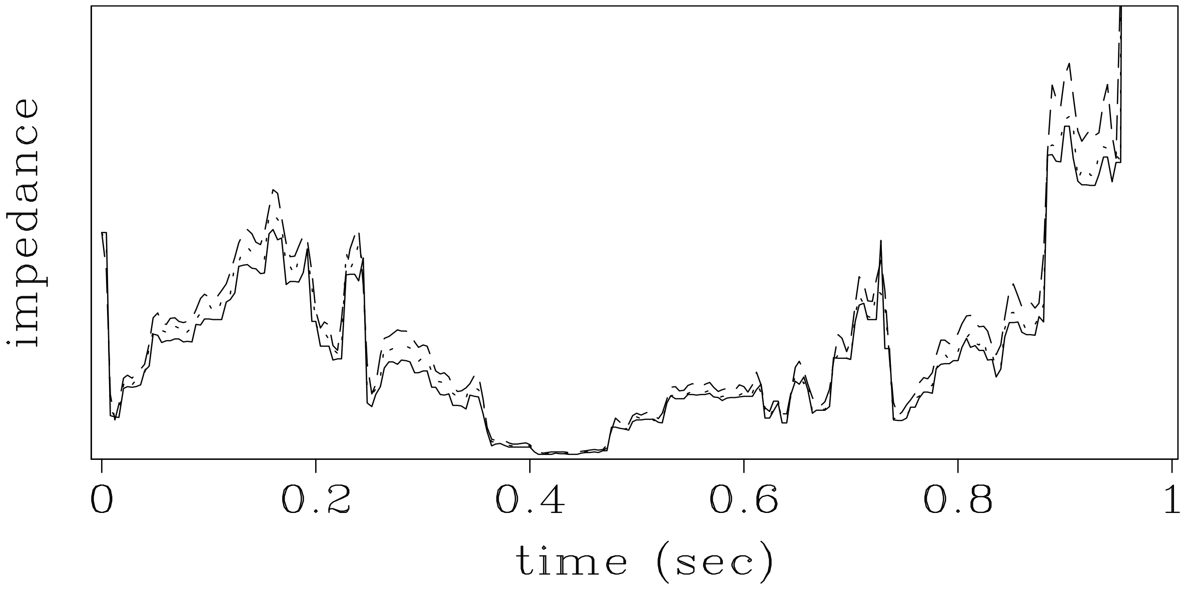

Figure 6: The **continuous** line is the true impedance obtained from the original synthetic reflectivity series, while the **dashed** and **dotted** lines correspond to the impedance obtained from the reflectivities retrieved by the LSI and ICP algorithms respectively. carlos1-imp [NR]

Figure 7 shows that using this operator with finite values of α is equivalent to the introduction of the damping factor in equation (7). Also we can see that the results obtained with small values of α are similar to those obtained with the predictive deconvolution. An L^p norm deconvolution can be formulated as an iterative, reweighted least-squares inversion with weighting factors given by $W(i) = \mid \Delta t(i) \mid^{p-2}$, where $\Delta t(i)$ are the residuals of the previous iteration (Darche, 1989). Since the value of the exponent α will directly affect the relative weighting of the residuals, we can consider the ICP decon as somehow equivalent to an L^∞ norm deconvolution.

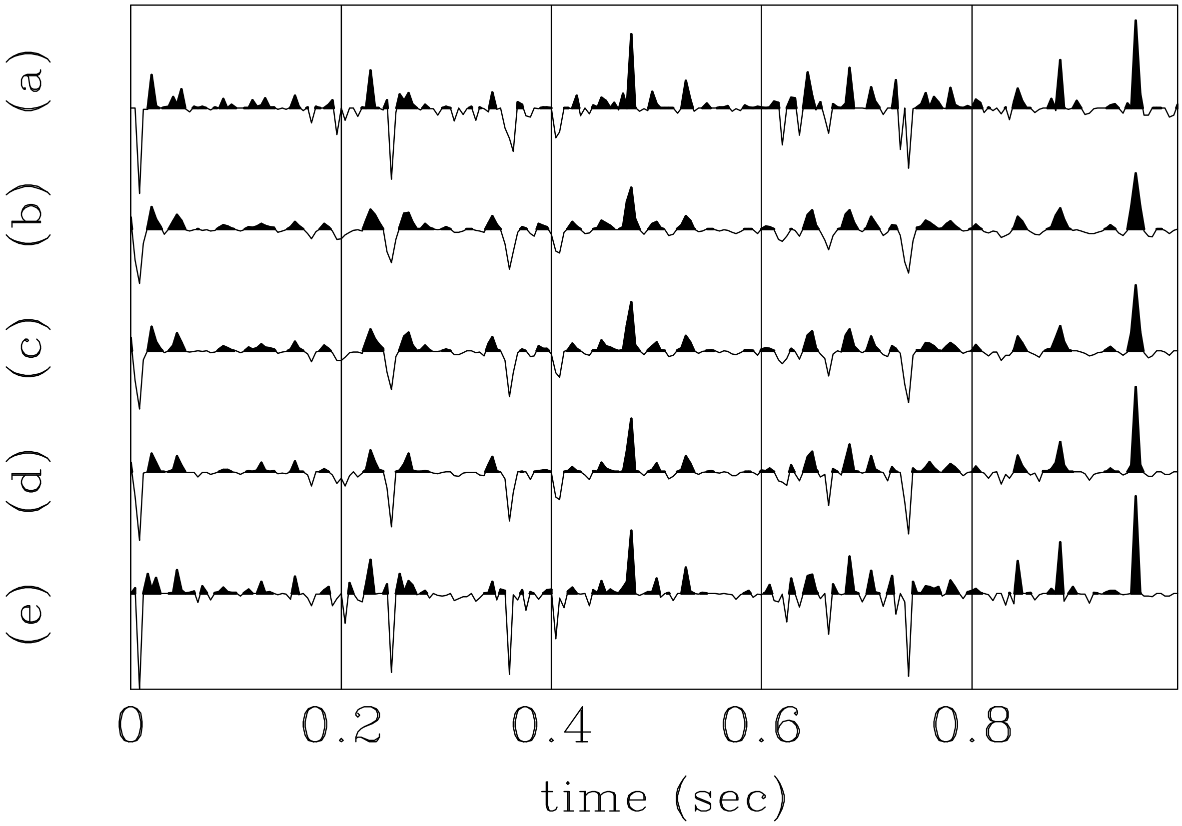

Figure 7: *(a)* Original reflectivity series. The other traces correspond to the results of the ICP algorithm using the generalized operator of equation (10) with different values of α: *(b)* $\alpha = 3$, *(c)* $\alpha = 5$, *(d)* $\alpha = 11$, and *(e)* $\alpha = \infty$. carlos1-knowt3 [NR]

SIMULTANEOUS ESTIMATION OF WAVELET AND REFLECTIVITIES

Wavelet estimation with a known reflectivity sequence

Although the convolution in equation (1) is commutative, the different spectra of **w** and **r** disallow us from using the same operator defined in equation (2) to retrieve the wavelet when the reflectivity sequence is completely known. However, if we start again from the ideal case of a sparse reflectivity sequence, it is possible to define an operator $\mathbf{Q_r}$ that retrieves the exact wavelet:

$$\mathbf{w} = \mathbf{Q_r}\{\mathbf{t}\}, \tag{12}$$

where the operator $\mathbf{Q_r}$ is defined according to

$$w_i = \frac{\sum_{j=0}^{n-i-1} r_j t_{j+i}}{\sum_{j=0}^{n-i-1} \mid r_j \mid^2} \qquad i = 0, 1, 2, ..., n-1. \tag{13}$$

This operator corresponds to a normalized correlation that properly handles edge effects because the norm in the denominator is evaluated over only the *active* part of $\mathbf{r}$.

A similar approach to the one described for reflectivity estimation can be taken for the wavelet estimation in the case of a non-sparse known reflectivity sequence. The iterative process is then described by

$$\mathbf{w^i} = \mathbf{w^{i-1}} + \mathbf{Q_r}\{\mathbf{t} - \mathbf{t^{i-1}}\} = \mathbf{w^{i-1}} + \mathbf{Q_r}\{\mathbf{t} - \mathbf{r} * \mathbf{w^{i-1}}\}. \tag{14}$$

Concatenating the two operators

Let $\mathbf{w^0}$ and $\mathbf{r^0}$ be some initial estimations of the wavelet and reflectivity sequence respectively. The data residuals can be described by

$$\begin{aligned}
\mathbf{\Delta t^0} &= \mathbf{t} - \mathbf{w^0} * \mathbf{r^0} \\
&= (\mathbf{w^0} + \mathbf{\Delta w}) * (\mathbf{r^0} + \mathbf{\Delta r}) - \mathbf{w^0} * \mathbf{r^0} \\
&= \mathbf{w^0} * \mathbf{\Delta r} + \mathbf{r^0} * \mathbf{\Delta w} + \mathbf{\Delta w} * \mathbf{\Delta r},
\end{aligned}$$

which can be linearized for small $\mathbf{\Delta w}$ and $\mathbf{\Delta r}$:

$$\mathbf{\Delta t^0} = \mathbf{w^0} * \mathbf{\Delta r} + \mathbf{r^0} * \mathbf{\Delta w}. \tag{15}$$

By applying the $\mathbf{P_{w^0}}$ operator to equation (15), we get

$$\mathbf{\Delta r} = \mathbf{P_{w^0}}\{\mathbf{\Delta t}\} - \mathbf{P_{w^0}}\{\mathbf{r^0} * \mathbf{\Delta w}\}.$$

If the sequence $\mathbf{r^0}$ is sufficiently sparse, the last term will involve the correlation between $\mathbf{w^0}$ and $\mathbf{\Delta w}$, which we can expect to be somewhat uncorrelated. The same reasoning can be applied to the operator $\mathbf{Q_{r^0}}$, resulting in the following recursion for reflectivities and waveform

$$\mathbf{r^i} = \mathbf{r^{i-1}} + \mathbf{P_{w^{i-1}}}\{\mathbf{\Delta t^{i-1}}\} \tag{16}$$

$$\mathbf{w^i} = \mathbf{w^{i-1}} + \mathbf{P_{r^{i-1}}}\{\mathbf{\Delta t^{i-1}}\}. \tag{17}$$

If we start the process with an initial estimation for the wavelet, then the initial estimation for the reflectivity sequence can be obtained when we apply $\mathbf{P_{w^0}}$ to the trace. As in most non-linear processes, the final solution depends on the initial choice for the wavelet. In all the next examples I used the minimum-phase wavelet corresponding to the smoothed spectrum of the trace as an initial estimation of the wavelet. Although the method has always converged for several different selections of the starting wavelet, an analytical proof that assures its convergence has not yet been derived.

Synthetic and real data examples

It is important to mention that the final solution depends not so much on the initial form of the wavelet, but on its initial phase. For the examples in Figures 8 and 9 the same final solution was reached when a delayed spike was used as the initial wavelet, as long as the delay was equal to the lag of the absolute maximum of the used wavelet.

The iterative algorithm described by equation (17) was applied to the same synthetic trace of the previous sections. Figure 8 compares the results of three different deconvolution approachs: predictive decon *(c)*; ICP decon using the minimum-phase wavelet corresponding to a smoothed version of the trace spectrum *(e)*; and convolution with the inverse filter of the same minimum-phase wavelet *(d)*. As we should expect, *(c)* and *(d)* are very similar because both methods are linear, and while one uses a minimum-phase wavelet, the other implicitly assumes the wavelet to be minimum-phase. Here again the ICP decon provides the sharper version of the reflectivity sequence since it keeps the same frequency distribution as the original series.

Figure 9 compares the true wavelet with the initial and final wavelets corresponding to the application of the ICP decon to the trace of Figure 8. The final estimated wavelet resembles the true wavelet, except by a constant time-shift, and some small oscillations on the tail.

Finally, I applied the ICP decon to a CMP gather recorded for British Petroleum in a deep-water environment of Alaska off-shore. Figure 10 shows *(a)* the unprocessed CMP gather, *(b)* the same data after predictive deconvolution, and *(c)* after the ICP deconvolution. The two deconvolution results are very similar, except by a slightly improved sharpness of the ICP deconvolution, as can be observed in the two reflections between 1.2 and 1.3 seconds; in *(a)* it is not possible to resolve the polarity of the reflections, while in *(b)* they were reduced to two main white events with small black side-lobs, and in *(c)* the black side-lobs have almost disappeared. We can also notice that in *(c)* the ocean floor reflection was also reduced to a single white event, without the black successor that appear in *(a)* and *(b)*.

I plan next, to extend the method to works in a multi-channel basis. Possible advantages of this extension are an improvement in the stability of the process, and an a more consistent estimation of the wavelet.

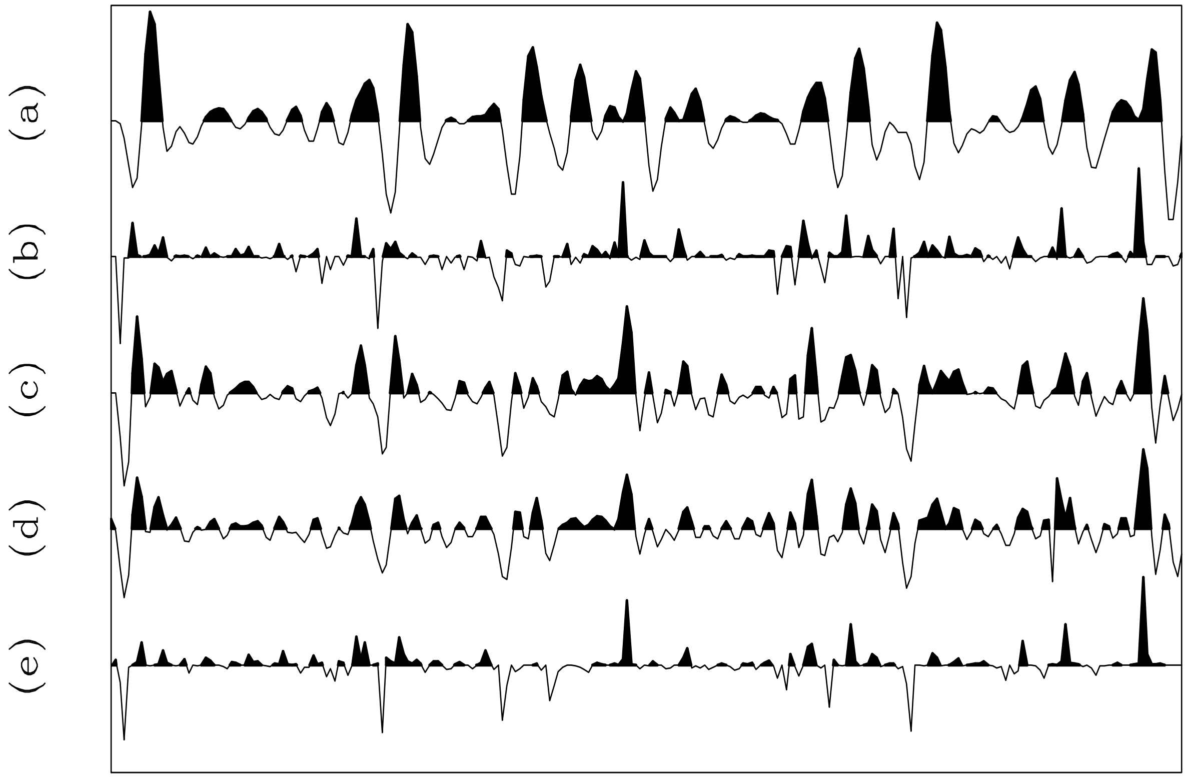

Figure 8: *(a)* Original trace and *(b)* original reflectivity series. The other traces correspond to the results of *(c)* predictive decon, *(d)* convolution with the inverse-wavelet filter, *(e)* and ICP decon. carlos1-unknow1 [NR]

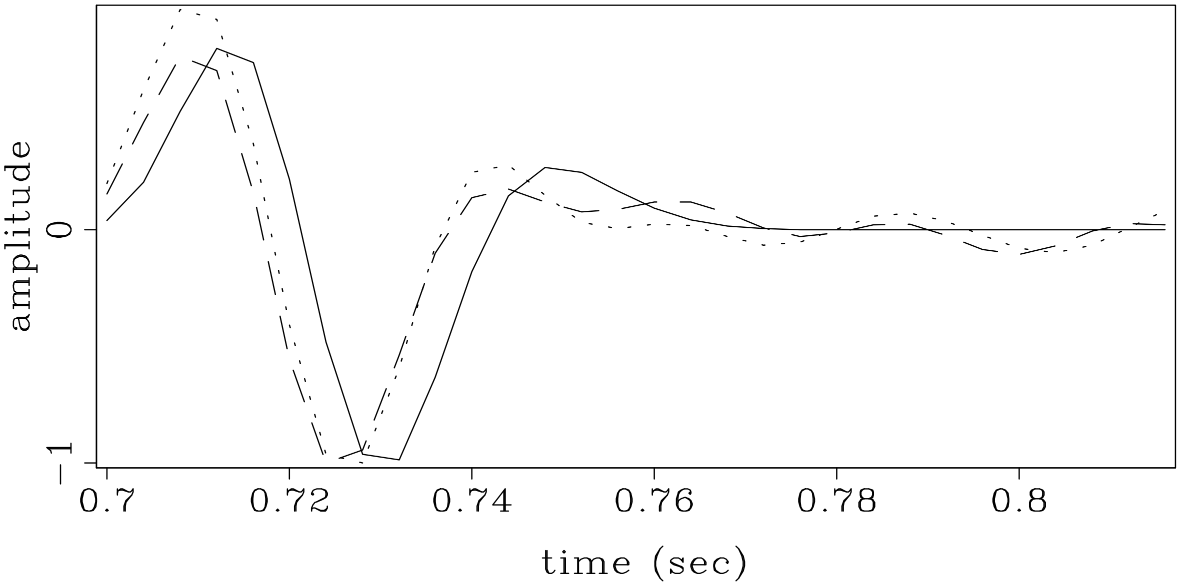

Figure 9: The **continuous** line is the true wavelet used to generate the trace of Figure 8-a, while the **dotted** and **dashed** lines correspond to the initial minimum-phase wavelet and the final wavelet estimated by the ICP algorithm. carlos1-unknow2 [NR]

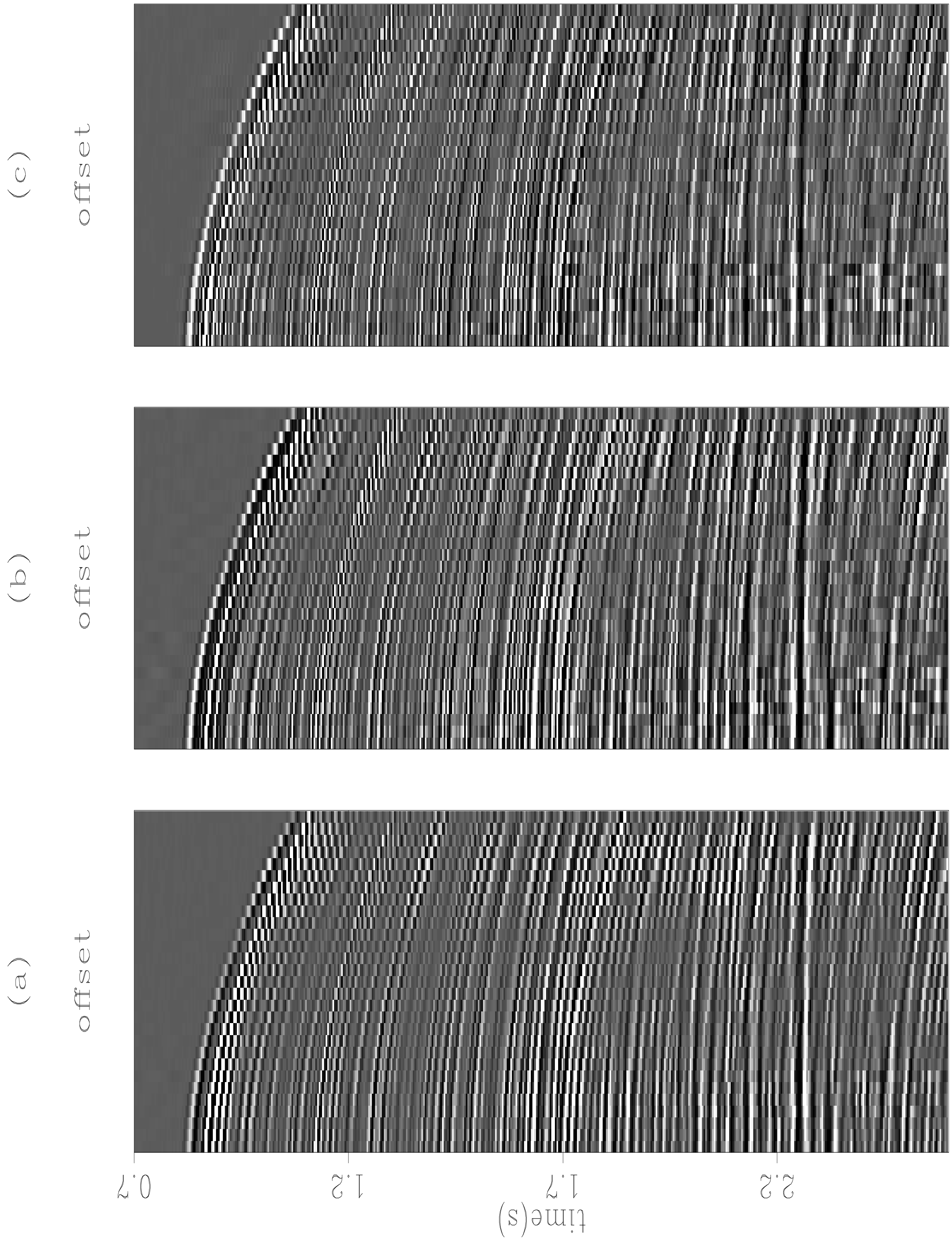

Figure 10: *(a)* CMP gather from Alaska offshore, *(b)* after predictive deconvolution, and *(c)* after ICP deconvolution. carlos1-realdat1 [NR]

CONCLUSIONS

When the wavelet is known, the ICP decon completely retrieves that components of the reflectivity series that share the same spectral region with the wavelet. In addition, the ICP algorithm keeps the same amplitude level in the whole frequency domain, resulting in a recovered time series that has the same sharpness as the original reflectivity sequence. When the wavelet is unknown the final result will depend on the choice of the initial wavelet, and when the minimum-phase equivalent of the trace is chosen to start the process, the ICP decon corresponds to a slightly sharper version of the predictive deconvolution.

Although a mathematical proof to assure convergence is still required, the method reached convergence in all the tests performed with the use of different choices for the starting wavelet.

REFERENCES

Claerbout, J.F., 1989, Time series analysis: Book 3 (still in preparation); also SEP–**61**, 391-414.

Darche, G., 1989, Iterative L_1 deconvolution: SEP–**61**, 281-301.

Debeye, H.W.J., and van Riel, P., 1989, L_p-norm deconvolution: 59*th* SEG Annual Meeting Abstracts, 1192-1194.

Jacobs, F.J., and van der Geest, P.A.G., 1988, Spiking band-limited traces with a relative entropy algorithm: 58*th* SEG Annual Meeting Abstracts, 723-726.

Wiggins, R.A., 1978, Minimum-entropy deconvolution: Geoexpl, **16**, 21-35.